Continuous Wave Terahertz Transmission Imaging of Nonmelanoma Skin Cancers

Cecil S. Joseph, PhD,[1*] Anna N. Yaroslavsky, PhD,[2,3] Victor A. Neel, MD, PhD,[3] Thomas M. Goyette, PhD,[1] and Robert H. Giles, PhD[1]

[1]*Submillimeter-Wave Technology Laboratory, University of Massachusetts Lowell, 175 Cabot St., Lowell, Massachusetts 01854*

[2]*Advanced Biophotonics Laboratory, University of Massachusetts Lowell, 175 Cabot St., Lowell, Massachusetts 01854*

[3]*Harvard Medical School, Massachusetts General Hospital, 55 Fruit Street, Boston, Massachusetts 02114*

Background and Objective: Continuous wave terahertz imaging has the potential to offer a safe, noninvasive medical imaging modality for delineating human skin cancers. Terahertz pulse imaging (TPI) has already shown that there is contrast between basal cell carcinoma and normal skin. Continuous-wave imaging offers a simpler, lower cost alternative to TPI. The goal of this study was to investigate the feasibility of continuous wave terahertz imaging for delineating skin cancers by demonstrating contrast between cancerous and normal tissue in transmission mode.

Materials and Methods: Two CO_2 optically pumped far-infrared molecular gas lasers were used for illuminating the tissue at two frequencies, 1.39 and 1.63 THz. The transmitted signals were detected using a liquid Helium cooled Silicon bolometer. Fresh skin cancer specimens were obtained from Mohs surgeries. The samples were processed and imaged within 24 hours after surgery. During the imaging experiment the samples were kept in pH-balanced saline to prevent tissue dehydration. At both THz frequencies two-dimensional THz transmission images of nonmelanoma skin cancers were acquired with spatial resolution of 0.39 mm at 1.4 THz and 0.49 mm at 1.6 THz. For evaluation purposes, hematoxylin and eosin (H&E) histology was processed from the imaged tissue.

Results: A total of 10 specimens were imaged and it was determined that for both frequencies, the areas of decreased transmission in the THz image correlated well with cancerous areas in the histopathology. Two negative controls were also imaged. The difference in transmission between normal and cancerous tissue was found to be approximately 60% at both frequencies, which suggests that contrast between normal and cancerous tissue at these frequencies is dominated by differences in water content.

Conclusions: Our results suggest that intraoperative delineation of nonmelanoma skin cancers using continuous-wave terahertz imaging is feasible. Lasers Surg. Med. 43:457–462, 2011. © 2011 Wiley-Liss, Inc.

Key words: continuous-wave terahertz imaging; skin-cancer imaging

INTRODUCTION

Nonmelanoma skin cancer is the most common form of cancer, with approximately 1 million new cases diagnosed each year. However, despite their common occurrence, they account for <0.1% of patient deaths caused by cancer [1]. An in vivo skin cancer imaging technique could provide a viable alternative to current methods of intraoperative visualization of cancer margins.

The terahertz region of electromagnetic spectrum extends from 30 to 3,000 μm (10–0.1 THz) and lies between the microwave and infrared regions. Terahertz radiation is nonionizing and medical applications of this frequency region are being explored [2–8]. Many biomolecules exhibit absorption in the terahertz region of the spectrum and biological effects of terahertz radiation are also being explored [9–11].

One of the restrictions of the imaging technique presented is the wavelength limited resolution. This limits the systems capability in terms of the accuracy of the margins it can provide during surgery. Working at higher frequencies can help improve the resolution; however, studies have shown that the difference in the real part of the refractive index between cancerous and normal skin decreases at higher frequencies in this region. The penetration depth of terahertz radiation at these frequencies is around 50 μm [11,12].

Studies show that there is a difference in bound and free water content between normal and cancerous tissue [13,14]. It was also reported that tryptophan content is increased in cancer [15,16]. Liquid water has a large attenuation coefficient and its absorption increases monotonically in this spectral region. Tryptophan has absorption bands with maxima at 1.4 and 1.8 THz. These absorption bands have been previously observed and assigned in literature [17]. Thus, tissue absorption

*Corresponding to: Dr. Cecil S. Joseph, Submillimeter-Wave Technology Laboratory, University of Massachusetts Lowell, 175 Cabot St., Lowell, MA 01854. E-mail: cecil_joseph@uml.edu

Accepted 17 May 2011
Published online 15 July 2011 in Wiley Online Library (wileyonlinelibrary.com).
DOI 10.1002/lsm.21078

characteristics at 1.4 THz depend on both water and tryptophan content. At 1.6 THz the tissue absorption characteristics depend on water content only, as tryptophan does not absorb significantly at this frequency. At 1.4 THz the refractive index of skin is 2 with an absorption coefficient of 250 cm^{-1} while at 1.6 THz the refractive index is 1.8 and the absorption coefficient is 300 cm^{-1} [12].

This study is ex vivo, transmission mode, and was designed to demonstrate transmission imaging of nonmelanoma skin cancers at two frequencies, 1.4 and 1.6 THz, using a continuous-wave (CW) terahertz imaging system. The tissue response at these frequencies was investigated and confirmed that contrast between cancerous and normal skin is observable. Fresh excisions of human skin cancer were used, and the terahertz images obtained were compared to hematoxylin and eosin (H&E) histology images of the samples. Due to the lack of commercially available continuous wave terahertz sources, most medical research in terahertz imaging thus far has been focused on terahertz pulsed imaging (TPI). Even though TPI has already been used to identify basal cell carcinoma (BCC) both ex vivo and in vivo [18], the source mechanism for the contrast in TPI images of BCC is not yet clearly understood [19]. The goal of this study was to investigate the feasibility of continuous wave terahertz imaging for delineating skin cancers by demonstrating contrast between cancerous and normal tissue in transmission mode.

MATERIALS AND METHODS

System Design and Construction

The sources used for this experiment were two CO_2 optically pumped far-infrared (FIR) gas lasers. The CO_2 and FIR lasers are custom designed and built at the Submillimeter-wave Technology Laboratory. The output power of these CO_2 lasers is in the range of 100–150 W. Tuning the output frequency of the CO_2 laser allows one to pump different transitions of the gas in FIR cell. Selecting the gas in the FIR cell and the tuning of the CO_2 laser to the appropriate pump frequency provides one with the ability to lase different frequencies in the terahertz region. These CO_2 lasers and the pumped FIR lasers have been described previously in literature [20].

The laser lines used were 1.39 THz (214.6 μm) and 1.63 THz (184.3 μm), horizontally polarized transitions in CH_2F_2, pumped by the 9R34 and 9R32 transitions of the CO_2 laser, respectively. The measured output powers were 370 and 31 mW at 1.39 and 1.63 THz, respectively.

A liquid helium cooled silicon bolometer manufactured by IRLabs was used as a detector. The noise equivalent power (NEP) of the detector was 1.13E−13 $W/Hz^{1/2}$ and the system responsivity was 2.75E+05 V/W. The bolometer had a response time of 5 milliseconds and the gain was 200. A crystalline quartz with Garnet powder window on the bolometer cut-off wavelengths below 100 μm.

Since the beams emerging from the FIR lasers is a few mm in diameter and expand rapidly as they propagate, an optical system was designed to focus both beams onto the same plane. Practically this means that their Rayleigh ranges should overlap in the imaging plane. Since the two frequencies are close, one was able to match the optical paths and generate comparable resolutions. Dielectric (glass) waveguides were placed at the output of the FIR lasers to obtain a Gaussian beam profile [21].

The waist is the radius of the Gaussian beam profile at the point at which the intensity drops to $1/e^2$ of its peak value. Figure 1 shows a schematic of the experimental layout. A detailed description of the imaging setup is provided elsewhere [22]. In brief, the two laser beams were collimated using a lens and focused onto the imaging plane using a short focal length off axis parabolic mirror. The beam waist of the 1.4 and 1.6 THz beams were

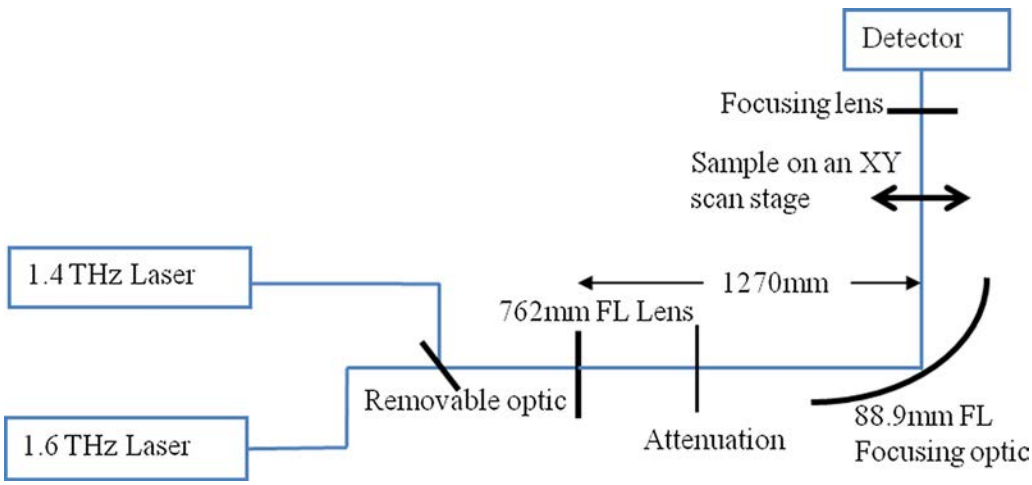

Fig. 1. Schematic of experimental layout.

measured to be 0.39 and 0.49 mm, respectively. A kinematic, removable mirror was employed to switch between the two frequencies. An automated two axis scan stage raster scanned the sample in the imaging plane. The resolution of the horizontal axis was set to 0.05 mm and the resolution of the vertical axis was 0.1 mm. The data collected by the bolometer was sent to a lock-in amplifier that had a time constant of 30 milliseconds. Data acquisition times for the images collected were determined by the speeds of the translation axes used for this experiment. The dwell time per point in the image was around 150 milliseconds. The motion control and data acquisition software was programmed using National Instruments LabView®.

Due to attenuation in the dielectric tube and the lens, the power incident on the sample plane was measured to be 25 mW at 1.4 THz and 7 mW at 1.6 THz. The system signal-to-noise ratio (SNR) using a lock-in amplifier was 68 dB for the 1.4 THz beam and 67 dB for the 1.6 THz beam.

Sample Preparation

The samples were prepared from fresh thick excess cancer specimens obtained within 2 hours from Mohs surgeries at Massachusetts General Hospital under an Institutional Review Board approved protocol. En-face skin sections were sliced to a thickness of 240 μm using a cryotome and mounted in between two slides of *z*-cut quartz. Using a 240 μm thick imaging spacer between the slides, the samples were kept in pH-balanced saline (pH 7.4). This insured that the samples did not dehydrate during the experiment. The tissue samples were imaged within 6 hours of being mounted. During the sample mounting procedure, several adjacent horizontal 5 μm slices were cut and stained for histology.

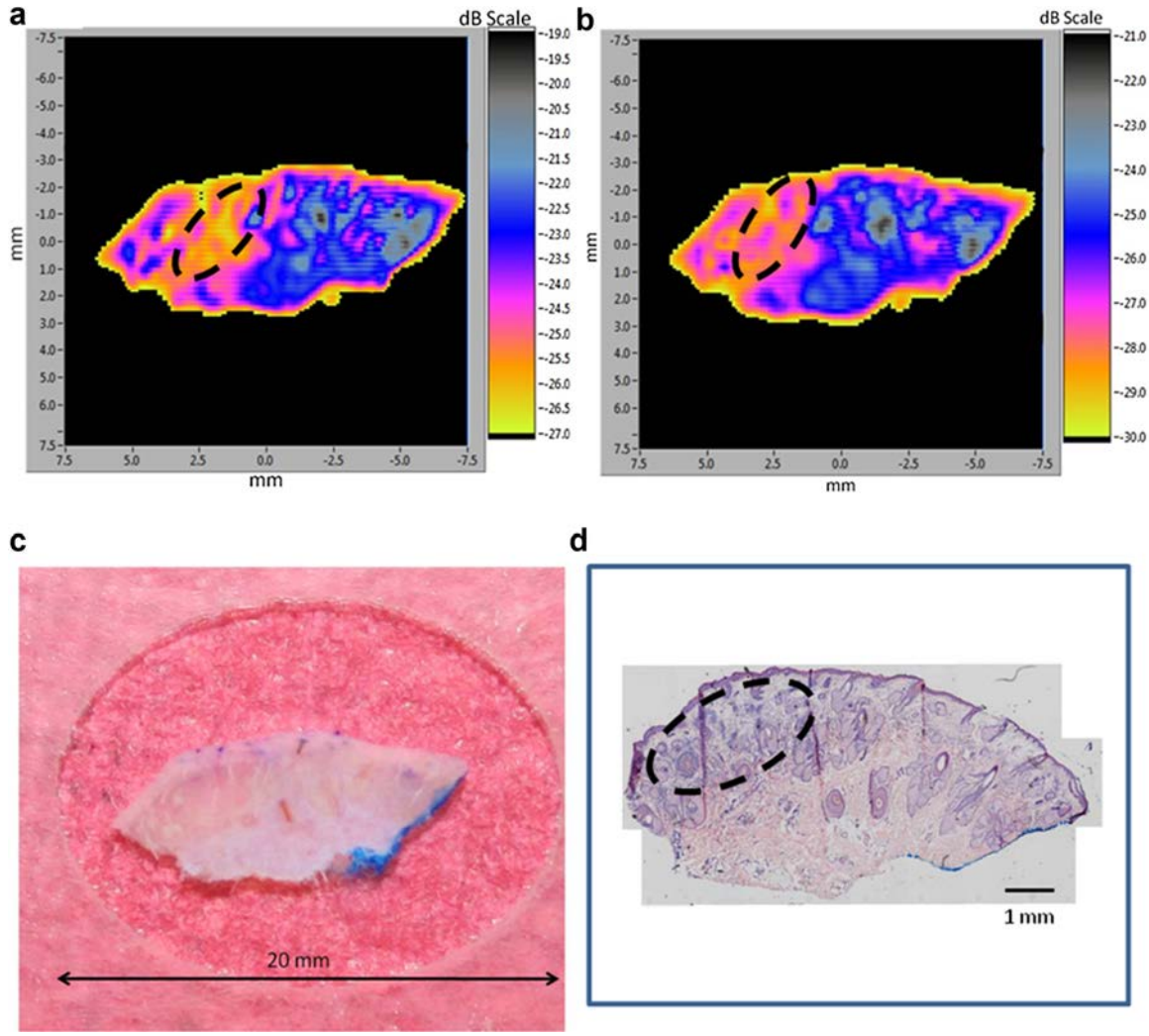

Fig. 2. **a**: Transmission image (104 THz) of sample in saline. **b**: Transmission image (1.6 THz) of sample in saline. **c**: Photograph of imaged sample sandwiched in between two slides of *z*-cut quartz. **d**: H&E histology of subsequent section.

Histology Processing

Horizontal sections were processed in the following way. Tissue was frozen in an optimal cutting temperature compound and processed in the standard *en-face* sectioning technique [23,24]. Five micron-thick sections were transferred to glass slides and stained with H&E. These frozen H&E sections were then compared to the terahertz images.

RESULTS

In Figure 2 example images of skin tissue with residual cancer are presented. Figure 2a,b shows terahertz transmission images of 240 μm thick sections of tissue at 1.4 and 1.6 THz, respectively. Figure 2c shows the digital photograph of the sample sandwiched in between two slides of *z*-cut quartz and Figure 2d shows the histology of the corresponding adjacent 5 μm slice of the sample. The cancerous region (BCC) is demarcated by the black dotted line in histology. The highly cellular area which appears medially to the outlined cancerous region comprises of sebaceous glands, hair follicles, and eccrine glands. In the terahertz images the black dotted line encircles areas of low transmission. The sample orientation with respect to histology was fixed using the blue surgeon's marker at the corner of the tissue section, visible in both the digital photograph (Fig. 2c) and the histology (Fig. 2d). The off-sample portion of the terahertz images was set to zero during post-processing and only contrast on the sample image was studied.

The transmission of the 1.4 THz beam through the sample assembly varies between −19 and −27 dB while the transmission of the 1.6 THz beam varies between −21 and −30 dB. Thus, the 1.6 THz beam is more severely attenuated through the sample as compared to the 1.4 THz beam. This is expected as the water content of skin is approximately 70%.

As one can see in Figure 2, the cancerous tissue area demarcated in the histology matches the areas of lower transmission demarcated in terahertz images fairly well. Decreased transmission in the cancerous region in the terahertz images indicates that the tumor responds differently to terahertz radiation in that area.

Figure 3a,b shows the difference between low transmittance (cancerous) and high transmittance (noncancerous) areas for the 10 samples measured.

It is observed that the transmission difference between normal and cancerous regions of the tissue is similar at both frequencies with the higher frequency being considerably more attenuated. At 1.4 THz, the transmittance averaged over normal areas of all 10 tissues investigated was found to be 0.0091 ± 0.006. At the same frequency, for cancerous areas the averaged transmittance was found to be 0.0033 ± 0.0012. At 1.6 THz, the averaged transmittance through normal areas of the samples was found to be 0.0021 ± 0.0012 while for cancerous areas the average transmittance was 0.0007 ± 0.0002.

There could be several reasons for higher standard deviations obtained from normal as compared to

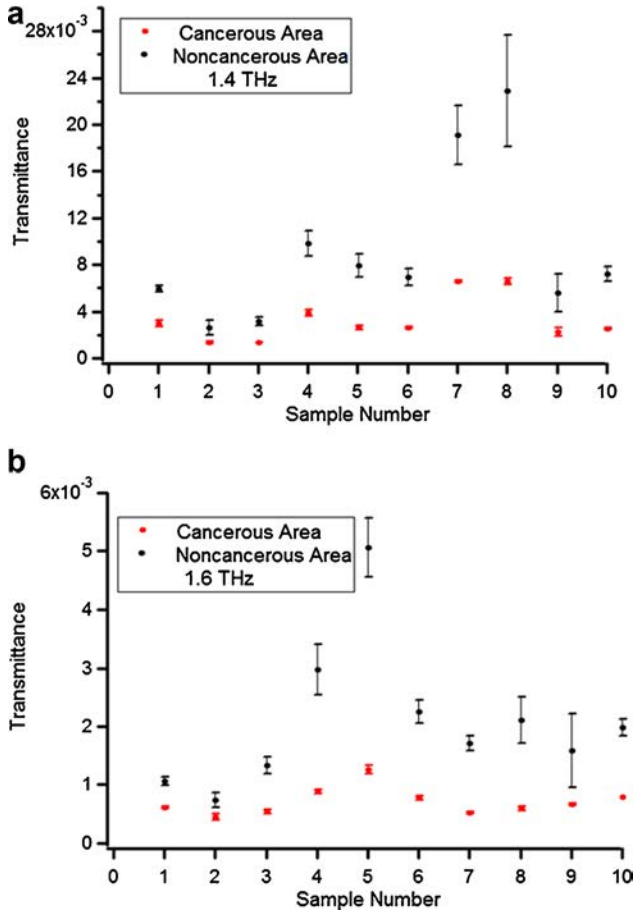

Fig. 3. Transmittance of identified cancerous and noncancerous areas on each sample at 1.4 THz (**a**) and 1.6 THz (**b**).

cancerous skin. Firstly, the thickness of different tissue samples may vary by few microns, which will result in observable transmittance differences. Another possible source of larger standard deviations in normal skin comes from averaging across all the samples that may have different hydration levels depending on the body site and variations between patients. In in vivo application, reference measurement of the adjacent normal skin will remedy the uncertainty in skin hydration. Another factor contributing to large standard deviations in normal skin, is that averaging over entire normal areas includes many types of structures, such as sebaceous glands, eccrine glands, hair follicles, etc.

Note that the relative transmittance difference across the samples, however, is fairly constant. And comparing cancerous areas to normal on the same tissue yields good specificity. In order to quantify this, the relative difference in transmitted intensity between cancerous and noncancerous areas of the same sample was calculated for each of the 10 samples measured.

The number is arrived at in the following manner for each sample, relative transmittance $= (T_{nc} - T_c)/T_{nc}$, where T_c is the averaged transmittance of a cancerous

TABLE 1. Relative Difference in Transmittance Between Cancerous and Noncancerous Areas at Both Measurement Frequencies for All 10 Samples

Sample number	Relative transmittance difference at 1.4 THz	Relative transmittance difference at 1.6 THz
1.	0.502008	0.423583
2.	0.502271	0.401606
3.	0.573178	0.587489
4.	0.601648	0.702258
5.	0.673932	0.752219
6.	0.618423	0.654626
7.	0.65317	0.696863
8.	0.712825	0.71755
9.	0.597368	0.577225
10.	0.645688	0.600729

area on the sample and T_{nc} is the averaged transmittance of a noncancerous area of the same specimen. This was done to calibrate out the effects of mounting and tissue variations. Table 1 shows the calculated relative transmittance differences for both measurement frequencies.

Averaging the relative transmittance difference across the 10 samples yields an average transmittance difference of $60.8 \pm 7\%$ at 1.4 THz and $61.1 \pm 12\%$ at 1.6 THz. While the contrast level at 1.6 THz appears to be greater than that at 1.4 THz, this difference is within the error of the measurement. As was mentioned above, tryptophan has an absorption peak at 1.4 THz, whereas water exhibits strong absorption at both frequencies. Therefore, it appears that difference in water content and/or state is the dominant source of contrast between tumor and normal skin, which can be employed for cancer demarcation.

DISCUSSION

A CW terahertz transmission imaging system capable of imaging human skin at two frequencies, 1.4 and 1.6 THz was developed and tested. The system's resolution was found to be 0.39 mm at 1.4 THz and 0.49 mm at 1.6 THz. The system SNR was also found to be of the order of 70 dB at both frequencies. Terahertz images of human skin samples were acquired and compared to sample histopathology. The analysis of the images indicates that the imaging system may be capable of registering transmission differences between nonmelanoma skin cancer and normal skin. Our results suggest that water absorption dominates tissue transmission characteristics. This is in agreement with other work in this area [12].

The SNR of the presented CW system exceeds the available SNR of pulsed systems operating in the same wavelength region by 10 dB and offers similar resolution [18]. The projected cost of a CW imaging system is considerably less than that of a pulsed system [3]. With further development, which includes using a coherent detection scheme, an opto-mechanical scanner and deployable source technology, the SNR is projected to increase by another 80 dB and image acquisition times can be minimized. The lower costs, coupled with the possibility of higher SNR and fast acquisition times, for CW systems stimulates further investigation of their potential for clinical applications. A pilot trial is underway that will establish the sensitivity and specificity of the CW terahertz imaging for skin cancer demarcation and demonstrate reflection modality terahertz imaging. This will serve as confirmation of the imaging system frequency and will establish the feasibility of the technique.

Data acquisition times for the images collected were determined by the speeds of the translation axes used for this experiment. The dwell time per point in the image was around 150 milliseconds. For the system presented here the limitation on acquisition time comes from both the translation of the sample across the image plane and the slow response of the bolometric detector. Future work will focus on building a reflectance terahertz CW imager capable of in vivo skin cancer imaging. This imager would utilize appropriate source technology, as a CO_2 pumped gas laser is not feasible for clinical applications, however, solid state devices can be used once it is established that frequency tunability is not desired. Also, integrating a diode based coherent detection scheme and an opto-mechanical scanner into the device will provide significant advantages in SNR and data acquisition time.

ACKNOWLEDGMENTS

The authors are grateful to the National Ground Intelligence Center, Charlottesville, VA, for the use of Government furnished Equipment at the Submillimeter-Wave Technology Laboratory, for carrying out this project. The authors are also grateful to Irina Tabatadze for cutting and processing sample histology.

REFERENCES

1. Skin cancer treatment PDQ. National Cancer Institute.
2. Berry E, Walker GC, Fitzgerald AJ, Zinov'ev NN, Chamberlain M, Smye SW, Miles RE, Smith MA. Do in vivo terahertz imaging systems comply with safety guidelines? J Laser Appl 2003;15:192–198.
3. Karpowicz N, Zhong H, Xu J, Lin K, Hwang J, Zhang X-C. Comparison between pulsed terahertz time-domain imaging and continuous wave terahertz imaging. Semiconductor Sci Tech 2005;20(7):S293–S299.
4. Chan WL, Deibel J, Mittleman DM. Imaging with terahertz radiation. Rep Prog Phys 2007;70:1325–1379.
5. Woodward RM, Wallace VP, Pye RJ, Cole BE, Arnone DD, Linfield EH, Pepper M. Terahertz pulse imaging of ex vivo basal cell carcinoma. J Invest Dermatol 2003;120:72–78.
6. Png GM, Choi JW, Ng BW-H, Mickan SP, Abbott D, Zhang X-C. The impact of hydration changes in fresh bio-tissue on THz spectroscopic measurements. Phys Med Biol 2008; 53(13):3501–3517.
7. Hoshina H, Hayashi A, Miyoshi N, Miyamaru F, Otani C. Terahertz pulsed imaging of frozen biological tissues. Appl Phys Lett 2009;94(12):123901.
8. Brun M-A, Formanek F, Yasuda A, Sekine M, Ando N, Eishii Y. Terahertz imaging applied to cancer diagnosis. Phys Med Biol 2010;55(16):4615–4623.
9. Pickwell E, Cole BE, Fitzgerald AJ, Pepper M, Wallace VP. In vivo study of human skin using pulsed terahertz radiation. Phys Med Biol 2004;49(9):1595–1607.

10. Wilmink GJ, Rivest BD, Roth CC, Ibey BL, Payne JA, Cundin LX, Grundt JE, Peralta X, Mixon DG, Roach WP. In vitro investigation of the biological effects associated with human dermal fibroblasts exposed to 2.52 THz radiation. Lasers Surg Med 2011;43(2):152–163.
11. Nazarov M, Shkurinov A, Tuchin VV, Zhang X-C. "Terahertz Tissue Spectroscopy and Imaging," Handbook of photonics for biomedical science, Ch. 23 (2010).
12. Wallace VP, Fitzgerald AJ, Pickwell E, Pye RJ, Taday PF, Flanagan N, Ha T. Terahertz pulsed spectroscopy of human basal cell carcinoma. Appl Spectrosc 2006;60(10):1127–1133.
13. Gniadecka M, Nielsen OF, Wulf HC. Water content and structure in malignant and benign skin tumours. J Mol Struct 2003;661:405–410.
14. Ross KFA, Gordon RE. Water in malignant tissue, measured by cell refractometry and nuclear magnetic resonance. J Microsc 1982;128:7–21.
15. Marshall WJ, Bangert SK. Clinical biochemistry: Metabolic and clinical aspects, 2nd edition. Philadelphia, PA,USA: Churchill Livingstone, Elsevier; 2008. p. 879.
16. Brackenridge CJ. The tyrosine and tryptophan content of blood serum in malignant disease. Clin Chim Acta 1960;5: 539–543.
17. Yu B, Zeng F, Yang Y, Xing Q, Chechin A, Xin X, Zeylikovich I, Alfano RR. Torsional vibrational modes of tryptophan studied by terahertz time-domain spectroscopy. Biophys J 2004;86:1649–1654.
18. Woodward RM, Cole BE, Wallace VP, Pye RJ, Arnone DD, Linfield EH, Pepper M. Terahertz pulse imaging in reflection geometry of human skin cancer and skin tissue. Phys Med Biol 2002;47:3853–3863.
19. Fitzgerald AJ, Wallace VP, Jimenez-Linan M, Bobrow L, Pye RJ, Purushotham AD, Arnone DD. Terahertz pulsed imaging of human breast tumors. Radiology 2006;239:533–540.
20. Goyette TM, Dickinson JC, Waldman J, Nixon WE. A 1.56 THz compact radar range for W-Band imagery of scale-model tactical targets. Proc SPIE 2000;4053:615–622.
21. Danylov AA, Waldman J, Goyette TM, Gatesman AJ, Giles RH, Linden KJ, Neal WR, Nixon WE, Wanke MC, Reno JL. Transformation of the multimode terahertz quantum cascade laser beam into a Gaussian, using a hollow dielectric waveguide. Appl Opt 2007;46(22):5051–5055.
22. Joseph CS, Yaroslavsky AN, Lagraves JL, Goyette TM, Giles RH. Dual-frequency continuous-wave terahertz transmission imaging of nonmelanoma skin cancers. Proc SPIE 2010;7601 (SPIE, Bellingham, WA 2010) 760104–760104-8.
23. Gross KG, Steinman HK, Rapini RP. editors. Mohs surgery: Fundamentals and techniques. St. Louis: Mosby, Inc.; 1999.
24. Mohs FE. Chemosurgery—A microscopically controlled method of cancer excision. Arch Surg 1941;42:279–295.